Deviations from Universality in the Transition from Quasiperiodicity to Chaos

Andrew Cumming and Paul S. Linsay
Department of Physics, Massachusetts Institute of Technology, Cambridge, Massachusetts 02139
(Received 12 March 1987)

We present experimental evidence for deviations from universality in the transition to chaos from quasiperiodicity in a nonlinear dynamical system. The dimension of the quasiperiodic set at the transition is 0.795 ± 0.005, not 0.87 as predicted by the standard model based on the circle map. We also deviate from predictions of the model at the golden mean: The power spectrum, tongue convergence rate, and spectrum of critical exponents, $f(\alpha)$, all differ from the theory.

PACS numbers: 05.45.+b, 03.40.−t

In recent years a standard model of the transition to chaos from quasiperiodicity in dynamical systems has been developed through the work of several groups based on the circle map,

$$X_{n+1} = X_n + \Omega - (K/2\pi)\sin(2\pi X_n). \quad (1)$$

The consequences of this model are thought to be universal, at least for any map which has a cubic inflection point. The first prediction of the model is that the quasiperiodic set becomes a fractal with a dimension of approximately 0.87 at the critical line,[1] the line at which the transition to chaos occurs. This is a global prediction in the sense that it is independent of winding number. The remaining three predictions also describe behavior at the critical line but are specialized to a winding number equal to the golden mean $\frac{1}{2}(\sqrt{5}-1)$, although they can be generalized to other winding numbers: (a) The time series of the dynamical system can be described by a curve of critical exponents,[2] $f(\alpha)$, which is related to the generalized dimensions of the time series.[3,4] (b) The bare winding numbers of the tongues which best approximate the golden mean scale as[5]

$$(\Omega_n - \Omega_{n+1})/(\Omega_{n+1} - \Omega_{n+2}) = -2.83\ldots. \quad (2)$$

(c) The power spectrum of the time series is self-similar.[5,6] Previous experiments have been in agreement with this model.[7]

The experimental apparatus used to test this model is a simple operational-amplifier relaxation oscillator[8] driven by a sine wave which can be varied in frequency and amplitude. The frequency of the free oscillation is near 252 kHz and is stable to a part in 10^5. The long-term drift measured over a period of 16 d is approximately 0.5 Hz/h. Extraneous noise from 60-Hz lines and other sources is eliminated by the operation of the oscillator from low-noise power supplies. The output of the circuit is filtered by a 500-kHz, five-pole Butterworth low-pass filter, digitized by a twelve-bit analog-to-digital converter, and then stored in a computer for further processing. Continuous time series of up to 32768 consecutive samples can be taken.

A section of the phase diagram of the oscillator as a function of the drive frequency and amplitude is shown in Fig. 1. The periodic zones are shaded and quasiperiodic and chaotic regions are blank. The winding number is indicated for several selected zones and increases monotonically from right to left. The structure above the critical line (the solid line) is different from the fine structure[9] of (1); in particular, it does not exhibit the forks characteristic of the circle map although a bump is observed above the critical line on the low-frequency edge of several of the larger tongues. Below the critical line, the time series is either quasiperiodic or periodic because of phase locking of the oscillator with the drive. Above the critical line we see only periodic or

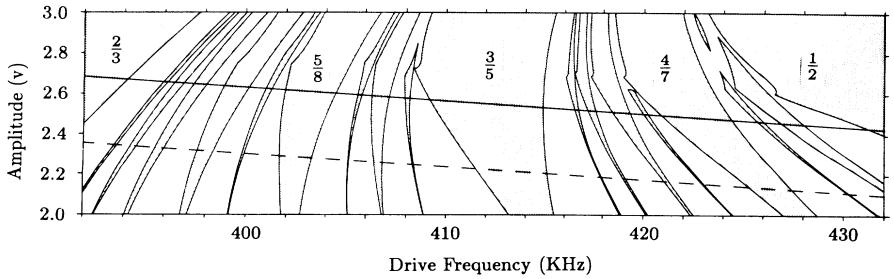

FIG. 1. Phase diagram of the driven relaxation oscillator between the $\frac{1}{2}$ and $\frac{2}{3}$ phase-locking tongues and bracketing the critical line (solid line). The bare winding number is defined as the oscillator frequency divided by the drive frequency. Only low-order phase lockings are shown.

chaotic response. In this region the transition to chaotic behavior from periodic motion is via a saddle-node bifurcation at the high-frequency side of a tongue. On the low-frequency side of each tongue, the transition to chaos is via a saddle-node bifurcation below the bump and via period doubling above the bump. We do not observe hysteresis for any transition.

Accurate determination of the critical line is necessary for a good measurement of the dimension of the quasiperiodic set at criticality. The most precise method we have found is observation of a change in the attractor as the transition occurs. Figures 2(a) and 2(b) show the attractor just below and just above the critical line. The appearance of chaos is obvious in Fig. 2(b). The apparent folding of the attractor at the lower left is due to the choice of projection. In fact, this is part of an open loop. Both the Lyapunov exponent and the dimension of the attractor were found to be too inaccurate and expensive of computer time to locate the critical line precisely, while the Fourier transform of the time series gave ambiguous results. A change in the attractor was used as a discriminant for the chaotic transition because, over the full length of the critical line, it was a sharper criterion than a change in the appearance of the power spectrum. Folding and breakup of the torus as evidence of the onset of chaos were generally apparent at lower amplitudes than any change in the power spectrum because of the extreme weakness of the chaos in this experiment. A chaotic spectrum was never found without folding and breakup of the attractor as well, whereas it was common to observe the reverse, evidence of chaos on the torus and a very clean Fourier transform.

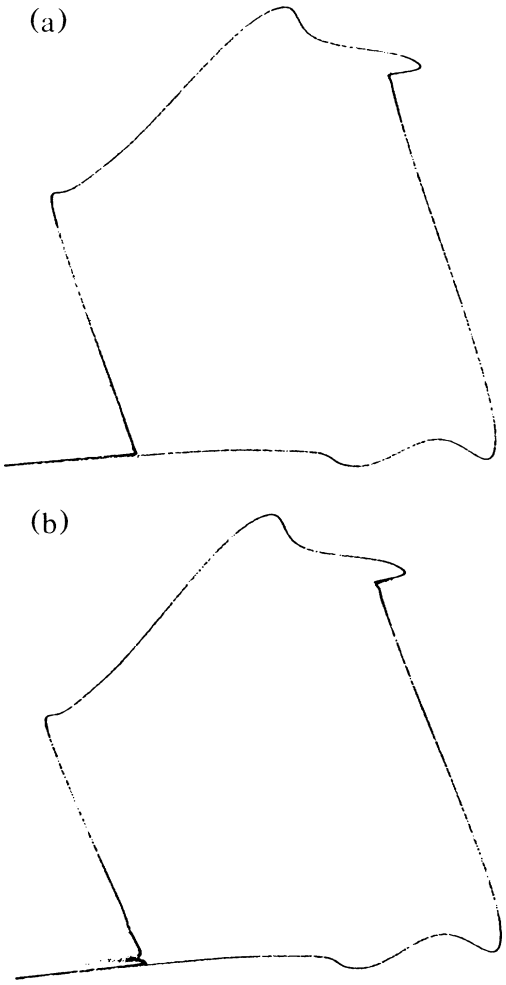

FIG. 2. Attractor along a line parallel to the low-frequency edge of the $\frac{1}{2}$ phase-locking zone, made by the projection of the sample voltage triplet, (V_n, V_{n+3}, V_{n+6}), onto the best-fit plane. V_n is the oscillator voltage sampled at the nth cycle of the drive. The attractor (a) 10 mV below the critical line, (b) 10 mV above the critical line.

Once the critical line was located, it was scanned automatically by computer and 333 tongues were found with widths as small as 1 Hz. The algorithm could not find tongues narrower than 10 Hz reliably, so only wider ones were used in the computation of dimension. The boundaries of the tongues, however, are accurate to within 1 Hz. The dimension, D, was computed from the formula[4]

$$\sum_i (S_i/S)^D = 1,$$

where the S_i are the distances between adjacent tongues and S is the distance between the $\frac{1}{1}$ and $\frac{1}{2}$ tongues. The dimension was computed as a function of all tongues that exceeded a certain width and then extrapolated to zero width. Using the 287 tongues wider than 10 Hz between the $\frac{1}{1}$ and $\frac{1}{2}$ phase-locking tongues, we have measured the dimension of the quasiperiodic set to be 0.795 ± 0.005. This value did not change if we included all tongues found. If the measurement of dimension is restricted to the piece of the critical line between either the $\frac{1}{1}$ and $\frac{1}{2}$ tongues or between the $\frac{1}{2}$ and $\frac{2}{3}$ tongues, the result is the same within errors. Local measurement

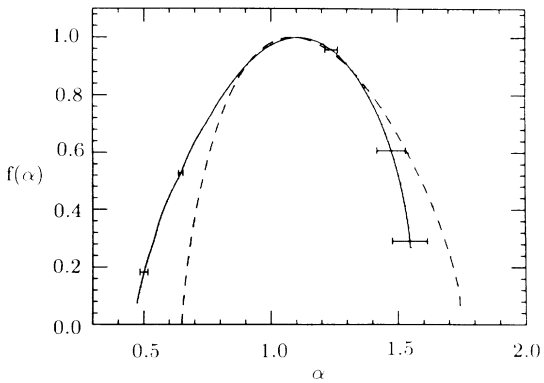

FIG. 3. Experimental measurement of $f(\alpha)$ (solid line) and computed value from (1) (dashed line).

of the dimension at the golden mean gave 0.75 ± 0.02. The dashed line in Fig. 2 is our best estimate of where the dimension of the quasiperiodic set would be 0.87 based on the above algorithm. Careful inspection of the attractor reveals no chaotic behavior in the vicinity of this line. Even though the quasiperiodic set at criticality does not have the dimension of the model, there still appears to be a complete devil's staircase of rational phase-locking zones there.

Turning to predictions of behavior at the critical line and at the golden mean we show the function $f(\alpha)$ computed from the time series in Fig. 3. In order to compute $f(\alpha)$, we first embedded the attractor in three dimensions to prevent it from crossing itself and then formed a smoothed attractor by averaging points locally to remove experimental noise. A normalized distance along the attractor, x $(0 \leq x \leq 1)$, was then computed for each datum by our projecting it onto the smoothed attractor. The quantities q and $d\tau/dq$ were then computed from the partition function[2]

$$\sum_{i=1}^{N} \frac{p_i^q}{l_i^\tau} = 1,$$

where the l_i are the distances between adjacent points on the attractor and the probabilities, $1/p_i$, were set equal to the number of points analyzed, N. The $f(\alpha)$ curves were then computed with use of the Legendre transformation,[2]

$$\alpha = d\tau/dq, \quad f(\alpha) = q\alpha - \tau.$$

The measured curve is the average of sixteen curves each calculated from a different time series 2048 points long. The experimental curve does not agree with the predictions of the theory, indicating that the spectrum of critical exponents, or equivalently, the set of generalized dimensions is different from the circle map (1).

A first-return map computed from the same smoothed attractor used to compute $f(\alpha)$ is shown in Fig. 4. The function is smooth with continuous derivatives and has no discontinuities. Careful inspection of the map reveals at least seven inflection points. The function of Eq. (2) at the golden mean did not converge but was found to switch between the two values -3.3 ± 0.1 and -2.7 ± 0.2 where we have used the center of the tongues for the values of the Ω_n.

The power spectrum of the driven oscillator at the golden mean and the onset of chaos is shown in Fig. 5. Seven generations of frequency scaling by the golden mean are displayed in the plot. The lowest-frequency components are slightly broadened because of a small amount of chaotic motion. There is some resemblance of this spectrum to the prediction of Ostlund *et al.*[6] We observe many of the subharmonic peaks, which are related by power laws because of the algebraic properties of the golden mean, but the relative amplitudes deviate considerably from the theory, in some cases by 2 orders of magnitude.

We have shown that there are deviations from universality in the transition to chaos from quasiperiodicity as determined by the dimension of the quasiperiodic set at the critical line. In the dynamical system we studied experimentally, the dimension is 0.795 ± 0.005, unlike previously studied systems which have a dimension of 0.87. The local predictions of the standard model at the golden mean of the shape of the $f(\alpha)$ curve, the scaling of the power spectrum, and the convergence rate of the tongues are also different in our experiment. Unlike the period-doubling route to chaos which has a unique transition to chaos with constants derivable from the logistic map,[10] the quasiperiodic route is associated with at least two sets of numbers. One set is well described by the circle map (1). It is unknown at this time whether the results of this experiment can be derived from a map.

We would like to thank A. Arneodo, J. Yorke, and

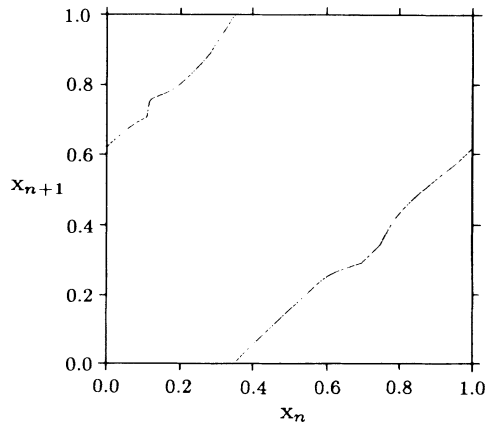

FIG. 4. First-return map at the critical line computed from the three-dimensional attractor, (V_n, V_{n+1}, V_{n+2}), with the winding number equal to the golden mean.

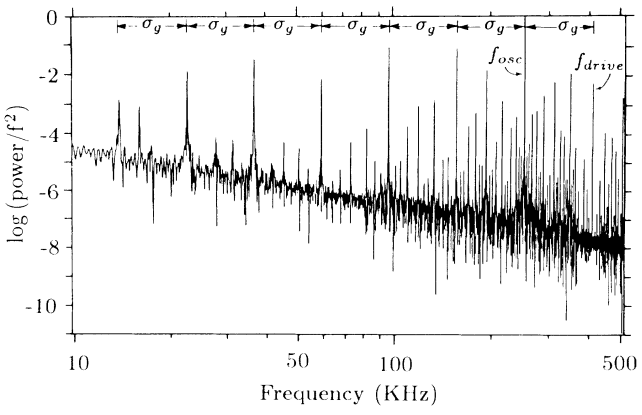

FIG. 5. Frequency-scaled power spectrum of the relaxation oscillator at the critical line with winding number equal to the golden mean.

S. Zaleski for helpful discussions. This work was supported by the U. S. Office of Naval Research.

[1]M. Jensen, P. Bak, and T. Bohr, Phys. Rev. Lett. **50**, 1637 (1983), and Phys. Rev. A **30**, 1960 (1984).

[2]T. Halsey *et al.*, Phys. Rev. A **33**, 1141 (1986).

[3]A. Renyi, *Probability Theory* (North-Holland, Amsterdam, 1970).

[4]H. Hentschel and I. Procaccia, Physica (Amsterdam) **8D**, 435 (1983).

[5]S. Shenker, Physica (Amsterdam) **5D**, 405 (1982).

[6]S. Ostlund, D. Rand, J. Sethna, and E. Siggia, Physica (Amsterdam) **8D**, 303 (1983); D. Rand *et al.*, Phys. Rev. Lett. **49**, 132 (1982).

[7]A. P. Fein, M. S. Heutmaker, and J. P. Gollub, Phys. Scr. **T9**, 79 (1985); J. Stavans, F. Heslot, and A. Libchaber, Phys. Rev. Lett. **55**, 596 (1985); J. Testa, Phys. Lett. **111A**, 243 (1985); M. Jensen *et al.*, Phys. Rev. Lett. **55**, 2798 (1985); S. Martin and W. Martienssen, Phys. Rev. Lett. **56**, 1522 (1986); E. Gwinn and R. Westerveldt, Phys. Rev. Lett. **57**, 1060 (1986).

[8]P. Horowitz and W. Hill, *The Art of Electronics* (Cambridge Univ. Press, Cambridge, England, 1980).

[9]L. Glass and R. Perez, Phys. Rev. Lett. **48**, 1772 (1982); J. Belair and L. Glass, Phys. Lett. **96A**, 113 (1983); M. Schell, S. Fraser, and R. Kapral, Phys. Rev. A **28**, 373 (1983).

[10]M. J. Feigenbaum, J. Stat. Phys. **19**, 25 (1978).